reward contingency automatically (6–16 times) without any indication to the monkey.

There were various types of error trial: failing to fixate the fixation point, breaking fixation before fixation offset, making a saccade in the wrong direction, and making a hypo- or hypermetric saccade in the right direction. Because it can be difficult to relate caudate pre-target activity to the various types of error trial, we limited our focus in the present paper to correct trials. Our behavioural procedure ensured that we had an equal amount of data from correct trials in the reward condition and those in the no-reward condition.

In the CST, there was a first fixation period of 1 s, followed by a brief presentation (100 ms) of a cue at 20° to the left or to the right. The monkey had to maintain his gaze at the fixation spot during a delay period of 1 s. The fixation spot then disappeared and the target was presented at the same position as the cue. In half of the trials, another spot appeared at the alternative position (distracter). The monkey had to make a saccade to the target position within 500 ms, and was rewarded with a drop of water for a correct saccade. After recording neurons in the CST (experiment 2), we re-applied the BST (experiment 1) for at least 80 trials to confirm the reproducibility of neuronal activity.

Data analysis

Pre-target neurons were defined as neurons that showed a statistically reliable increase in the spike count -1.5 s to 0 s before target onset ('pre-target window') as compared with the spike count -3 s to -1.5 s before target onset. All pair-wise comparisons were evaluated by two-tailed t-tests, $P < 0.01$. We used the Bonferroni procedure to correct for family-wise error with multiple t-tests. To quantify the separation of population distributions from contralateral versus ipsilateral conditions, we calculated the area under the ROC in a sliding window of 200 ms.

To test the adaptation of saccade latency and pre-target activity to a reversal of position-reward contingency, we compared the second trial after a reversal against the third trial after a reversal (test 1). We also compared the second trial after a reversal against the pooled data from the sixth to twentieth trial (test 2). Both tests consisted of paired two-tailed t-tests on the mean data from individual neurons. Adaptation was judged complete if there was no significant difference between the measures. Tests 1 and 2 produced similar results in all cases.

For comparison between the two tasks (BST versus CST), we considered the neuronal activity from -500 to 0 ms before target onset in both tasks, in the computation of absolute firing rates as well as ROC areas.

1. Amador, N., Schlag-Rey, M. & Schlag, J. Reward-predicting and reward-detecting neuronal activity in the supplementary eye field. *J. Neurophysiol.* **84,** 2166–2170 (2000).
2. Kobayashi, S., Lauwereyns, J., Koizumi, M., Sakagami, M. & Hikosaka, O. Influence of reward expectation on visuospatial processing in macaque lateral prefrontal cortex. *J. Neurophysiol.* **87,** 1488–1498 (2002).
3. Leon, M. I. & Shadlen, M. N. Effect of expected reward magnitude on the response of neurons in the dorsolateral prefrontal cortex of the macaque. *Neuron* **24,** 415–425 (1999).
4. Tremblay, L. & Schultz, W. Relative reward preference in primate orbitofrontal cortex. *Nature* **398,** 704–708 (1999).
5. Watanabe, M. Reward expectancy in primate prefrontal neurons. *Nature* **382,** 629–632 (1996).
6. Rolls, E. T. *The Brain and Emotion* (Oxford Univ. Press, New York, 1999).
7. Platt, M. L. & Glimcher, P. W. Neural correlates of decision variables in parietal cortex. *Nature* **400,** 233–238 (1999).
8. Hikosaka, O., Sakamoto, M. & Usui, S. Functional properties of monkey caudate neurons. III. Activities related to expectation of target and reward. *J. Neurophysiol.* **61,** 814–832 (1989).
9. Kawagoe, R., Takikawa, Y. & Hikosaka, O. Expectation of reward modulates cognitive signals in the basal ganglia. *Nature Neurosci.* **1,** 411–416 (1998).
10. Schultz, W., Apicella, P., Scarnati, E. & Ljungberg, T. Neuronal activity in monkey ventral striatum related to the expectation of reward. *J. Neurosci.* **12,** 4595–4610 (1992).
11. Schultz, W., Dayan, P. & Montague, P. R. A neural substrate of prediction and reward. *Science* **275,** 1593–1599 (1997).
12. Bindra, D. Neuropsychological interpretation of the effects of drive and incentive-motivation on general activity and instrumental behaviour. *Psychol. Rev.* **75,** 1–22 (1968).
13. Dickinson, A. & Baleine, B. Motivational control of goal-directed action. *Anim. Learn. Behav.* **22,** 1–18 (1994).
14. Watanabe, M. *et al.* Behavioral reactions reflecting differential reward expectations in monkeys. *Exp. Brain Res.* **140,** 511–518 (2001).
15. Apicella, P., Scarnati, E., Ljungberg, T. & Schultz, W. Neuronal activity in monkey striatum related to the expectation of predictable environmental events. *J. Neurophysiol.* **68,** 945–960 (1992).
16. Rolls, E. T., Thorpe, S. J. & Maddison, S. P. Responses of striatal neurons in the behaving monkey. I. Head of the caudate nucleus. *Behav. Brain Res.* **7,** 179–210 (1983).
17. Hikosaka, O., Sakamoto, M. & Usui, S. Functional properties of monkey caudate neurons. I. Activities related to saccadic eye movements. *J. Neurophysiol.* **61,** 780–798 (1989).
18. Kawaguchi, Y., Wilson, C. J. & Emson, P. C. Projection subtypes of rat neostriatal matrix cells revealed by intracellular injection of biocytin. *J. Neurosci.* **10,** 3421–3438 (1990).
19. Fisher, R. S., Buchwald, N. A., Hull, C. D. & Levine, M. S. The GABAergic striatonigral neurons of the cat: Demonstration by double peroxidase labeling. *Brain Res.* **398,** 148–156 (1986).
20. Hikosaka, O. & Wurtz, R. H. Visual and oculomotor functions of monkey substantia nigra pars reticulata. III. Memory-contingent visual and saccade responses. *J. Neurophysiol.* **49,** 1268–1284 (1983).
21. Lauwereyns, J. *et al.* Feature-based anticipation of cues that predict reward in monkey caudate nucleus. *Neuron* **33,** 463–473 (2002).
22. Takikawa, Y., Kawagoe, R. & Hikosaka, O. Reward-dependent spatial selectivity of anticipatory activity in monkey caudate neurons. *J. Neurophysiol.* **87,** 508–515 (2002).
23. Rescorla, R. A. & Wagner, A. R. in *Classical Conditioning II: Current Research and Theory* (eds Black, A. H. & Prokasy, W. F.) 64–99 (Appleton Century Crofts, New York, 1972).
24. Basso, M. A. & Wurtz, R. H. Modulation of neuronal activity by target uncertainty. *Nature* **389,** 66–69 (1997).
25. Dorris, M. C. & Munoz, D. P. Saccadic probability influences motor preparation signals and time to saccadic initiation. *J. Neurosci.* **18,** 7015–7026 (1998).
26. Hikosaka, O., Kawagoe, R. & Takikawa, Y. Role of the basal ganglia in the control of purposive saccadic eye movements. *Physiol. Rev.* **80,** 953–978 (2000).
27. Ikeda, T., Takikawa, Y. & Hikosaka, O. Visuo-motor and anticipatory activities of monkey superior colliculus neurons are modulated by reward. *Soc. Neurosci. Abstr.* **27,** 59.1 (2001).
28. Sato, M. & Hikosaka, O. Role of primate substantia nigra pars reticulata in reward-oriented saccadic eye movement. *J. Neurosci.* **22,** 2363–2373 (2002).

Competing interests statement

The authors declare that they have no competing financial interests.

Correspondence and requests for materials should be addressed to O.H. (e-mail: oh@lsr.nei.nih.gov).

Post-translational disruption of dystroglycan–ligand interactions in congenital muscular dystrophies

Daniel E. Michele*, Rita Barresi*, Motoi Kanagawa*, Fumiaki Saito*, Ronald D. Cohn*, Jakob S. Satz*, James Dollar†, Ichizo Nishino‡, Richard I. Kelley§, Hannu Somer‖, Volker Straub*, Katherine D. Mathews¶, Steven A. Moore# & Kevin P. Campbell*

* *Howard Hughes Medical Institute, Department of Physiology and Biophysics, and Department of Neurology; ¶ Department of Pediatrics; and # Department of Pathology, University of Iowa, Iowa City, Iowa 52242-1101, USA*
† *Department of Pathology, Albany Medical College, Albany, New York 12208, USA*
‡ *Department of Neuromuscular Research, National Institute of Neuroscience, Tokyo 187-8502, Japan*
§ *Kennedy Krieger Institute, John Hopkins University, Baltimore, Maryland 21205, USA*
‖ *Department of Neurology, Helsinki University Hospital, 00029 HUS Helsinki, Finland*

Muscle–eye–brain disease (MEB) and Fukuyama congenital muscular dystrophy (FCMD) are congenital muscular dystrophies with associated, similar brain malformations[1,2]. The FCMD gene, *fukutin*, shares some homology with *fringe*-like glycosyltransferases, and the MEB gene, *POMGnT1*, seems to be a new glycosyltransferase[3,4]. Here we show, in both MEB and FCMD patients, that α-dystroglycan is expressed at the muscle membrane, but similar hypoglycosylation in the diseases directly abolishes binding activity of dystroglycan for the ligands laminin, neurexin and agrin. We show that this post-translational biochemical and functional disruption of α-dystroglycan is recapitulated in the muscle and central nervous system of mutant myodystrophy (*myd*) mice. We demonstrate that *myd* mice have abnormal neuronal migration in cerebral cortex, cerebellum and hippocampus, and show disruption of the basal lamina. In addition, *myd* mice reveal that dystroglycan targets proteins to functional sites in brain through its interactions with extracellular matrix proteins. These results suggest that at least three distinct mammalian genes function within a convergent post-translational processing pathway during the biosynthesis of dystroglycan, and that abnormal dystroglycan–ligand interactions underlie the pathogenic mechanism of muscular dystrophy with brain abnormalities.

Dystroglycan is the central protein in the dystrophin–glyco-protein complex (DGC), linking dystrophin in the intracellular cytoskeleton to proteins in the extracellular matrix[5–7]. The biosynthesis of dystroglycan involves cleavage to generate the transmembrane β-dystroglycan (β-DG), which binds to the extracellular α-DG, both of which undergo extensive glycosylation[8,9]. Despite the known involvement of DGC proteins in muscular dystrophies, mutations in dystroglycan have not been identified[10–14]. In mice, disruption of the *DAG1* gene results in embryonic lethality, and normal dystroglycan expression seems to be essential for organization of basement membranes[15,16]. We characterized dystroglycan protein localization in muscle biopsies of four MEB patients and three FCMD patients with a panel of dystroglycan antibodies. Both MEB and FCMD patients showed normal sarcolemma expression of β-DG (Fig. 1a). However, staining with monoclonal antibodies IIH6 and VIA4-1 failed to detect α-DG (Fig. 1a). To determine whether any portion of α-DG was expressed at the sarcolemma, biopsies were stained with a polyclonal α-DG antibody, GT20ADG (see Methods), which showed normal localization (Fig. 1a). These results indicate that α-DG is expressed at the membrane but that the epitopes for the monoclonal antibodies are specifically disrupted in MEB and FCMD patients.

The epitope for IIH6 on α-DG can be disrupted *in vitro* by deglycosylation of α-DG[7], suggesting that α-DG may be abnormally glycosylated in MEB and FCMD patients. Western blots of glyco-proteins enriched with wheat germ agglutinin (WGA) agarose showed similar levels of β-DG expression, but no α-DG protein was detected with monoclonal antibodies IIH6 and VIA4-1 in MEB and FCMD patients (Fig. 1b, c). However, core α-DG polyclonal antibody showed that α-DG is expressed in MEB and FCMD patients at levels similar to control human muscle. Significantly, a reduction in relative molecular mass (M_r) of more than 50,000 (50K) in α-DG occurs in FCMD and MEB. More than half of the M_r of α-DG in normal muscle is glycoconjugates, and most of these glycoconjugates seem to be lost in both diseases. Interestingly, most α-DG migrates at similar M_r in FCMD and MEB, suggesting that the mutated genes associated with these two diseases might produce proteins that participate within the same enzymatic pathway, ultimately resulting in the transfer of sugars to α-DG. The rest of the components of the DGC, including dystrophin and the sarcoglycans, are normally expressed and glycosylated at the sarcolemmal membrane in MEB and FCMD (not shown).

Dystroglycan serves as a receptor for a variety of extracellular ligands, such as laminin[8], agrin[17,18] and neurexin[19], in muscle, neuromuscular junctions, nerve and brain. Full chemical deglyco-sylation of α-DG *in vitro* can disrupt laminin binding activity[7,19]. Therefore, we performed ligand overlay assays using laminin, neurexin and agrin on blots of WGA-enriched MEB and FCMD muscle (Fig. 2a, b). In muscle from MEB patients, ligand-binding activity of laminin, neurexin and agrin are each markedly diminished. Interestingly, in MEB patients the small amount of residual binding of ligands occurs in a dystroglycan species with higher M_r than most α-DG expressed. We suggest that a small amount of proper glycosylation occurs in the presence of mutated POMGnT1,
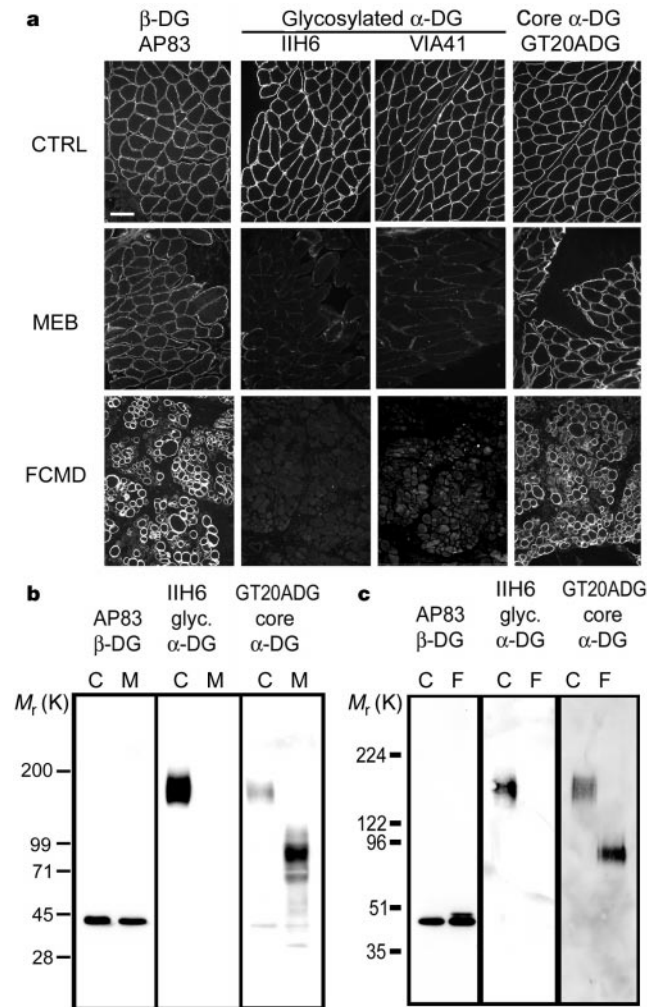

Figure 1 Post-translational modification of dystroglycan in MEB and FCMD.
a, Immunofluorescence localization of dystroglycan in biopsies of normal muscle (CTRL) and muscle of MEB and FCMD patients, using antibodies against β-DG, glycosylated α-DG, and α-DG core protein. Data shown are representative of all four MEB and all three FCMD patients. Scale bar, 100 μm. **b**, **c**, Immunoblot analyses of age-matched normal (C) and MEB patient (M, **b**) and FCMD patient (F, **c**) WGA-enriched total muscle glycoproteins.
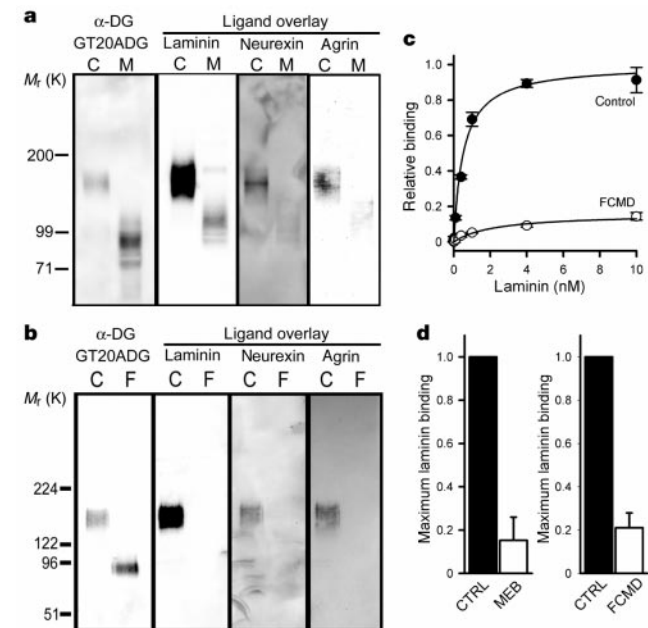

Figure 2 Dystroglycan–ligand interactions in MEB and FCMD. **a**, **b**, Ligand overlay assays on age-matched control (C) and MEB patient (M, **a**) and FCMD patient (F, **b**) WGA-enriched muscle homogenates using murine EHS laminin, neurexin fusion protein and recombinant rat agrin. **c**, Representative assay of solid-phase laminin-binding activity from control and FCMD muscle. Data are mean ± s.d. of triplicate samples fitted to a one-site model using the equation $A = B_{max}x/(K_d + x)$. **d**, Maximum laminin-binding activity in MEB ($n = 2$) and FCMD ($n = 3$) WGA glycoproteins relative to age-matched control muscle (CTRL). Data are mean ± s.e.m.

due either to residual enzymatic activity or to a secondary, partially compensatory enzyme. In FCMD patients, no binding of laminin, neurexin and agrin to α-DG is detected (Fig. 2b). To quantify the total ligand-binding activity of intact (non-denatured) α-DG, we performed solid-phase laminin-binding assays of WGA-enriched protein fractions from MEB, FCMD and age-matched control muscle (Fig. 2c, d). Nonspecific binding was calculated by the chelation of calcium with EDTA, which disrupts the laminin–α-DG interaction[7]. The quantitative solid-phase assays show a reduction of more than 80% in total high-affinity laminin-binding activity in MEB and FCMD muscle glycoproteins (Fig. 2d). Surprisingly, a small amount of residual binding activity remained in FCMD samples despite no activity by overlay assay (Fig. 2b, d). However, this residual activity in FCMD patients is insensitive to inhibition by the α-DG-blocking antibody IIH6, indicating that dystroglycan in FCMD is incapable of binding ligand (not shown). Total laminin-binding activity in age-matched control muscle was 80% inhibited by IIH6 (not shown). Because the residual high-affinity binding in FCMD is also insensitive to Arg-Gly-Asp (RGD) peptides (integrin inhibition, not shown), we suggest that this binding activity is due either to laminin in the preparation, or to an unknown, developmentally regulated laminin receptor in muscle. Thus, the lack of full glycosylation of α-DG in MEB and FCMD patients significantly disrupts the interactions of α-DG with extracellular matrix ligands known to be present in muscle, eye and brain.

The results in FCMD and MEB patients suggest that post-translational disruption of dystroglycan–ligand interactions may be a common mechanism for muscular dystrophy with brain abnormalities. A mutation in the *LARGE* gene, which encodes a putative *N*-acetyl-glucosamine glycosyltransferase, has been linked to the muscular dystrophy phenotype in the *myd* mouse[20]. In that study, muscle from *myd* mice showed a reduction in VIA4-1-reactive α-DG, but 'core antibodies' did not demonstrate any shift in the M_r of α-DG[20]. Furthermore, no brain abnormalities have been reported in *myd* mice, suggesting that the effect of this putative enzyme to cause muscular dystrophy may be through a different mechanism or different receptor than in MEB and FCMD patients. We found that fully glycosylated α-DG was localized in muscle sarcolemma and astrocyte foot processes surrounding microvessels and abutting the glia limitans in the brain of wild-type mice (Fig. 3a). In addition, IIH6-reactive α-DG was found concentrated in puncta surrounding cerebellar Purkinje cell soma and throughout the molecular layer of cerebellum (Fig. 3a). In the *myd* mouse, IIH6-reactive α-DG in muscle and brain was not detected in any of these sites (Fig. 3a). IIH6-reactive α-DG is also expressed in the tissues of the eye: extra-ocular muscle membranes, retina inner limiting membranes, foot processes surrounding microvessels, and puncta in the outer plexiform layer (not shown). In the *myd* mouse, IIH6-reactive dystroglycan is absent from all of these sites, and although retinal neuronal layering appears grossly normal, extra-ocular muscle shows dystrophic features (not shown).

Western blotting of WGA-enriched homogenates from *myd* muscle and brain showed a biochemical phenotype remarkably similar to that of WGA-enriched MEB and FCMD patient muscle glycoproteins (Figs 1b, c and 3b). β-DG is normally expressed and glycosylated in *myd* muscle and brain, but α-DG reactive to IIH6 (Fig. 3b) and VIA4-1 (not shown) is absent. Core α-DG antibodies show that α-DG is expressed in *myd* muscle and brain but reveal a decrease in α-DG M_r similar to that of FCMD and MEB patients. The specificity of this glycosylation defect is indicated by normal expression of DGC proteins at the sarcolemma, normal sarcolemma lectin staining, and normal glycosylation of the sarcoglycans in *myd*
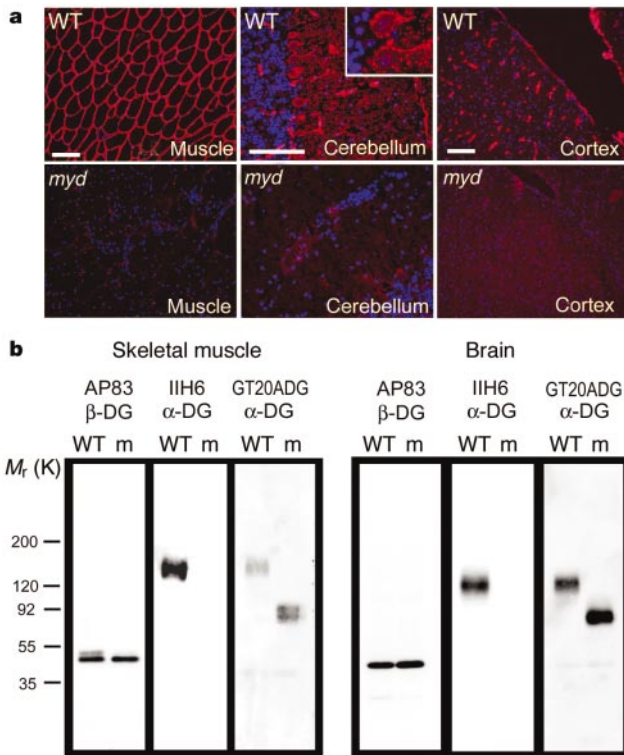

Figure 3 Post-translational modification of dystroglycan in *myd* muscle and brain. **a**, IIH6 immunolocalization in wild-type (WT) and *myd* muscle and brain (red). IIH6 epitopes on α-DG are lost in *myd* muscle sarcolemma and in astrocyte foot processes, and puncta in molecular layer (inset) in *myd* mice. Counterstain is 4,6-diamidino-2-phenylindole (DAPI), which labelled nuclei (blue). Scale bar, 100 μm. **b**, Western blot analysis of dystroglycan expression in WGA-enriched homogenates of wild-type and *myd* (m) muscle and brain.
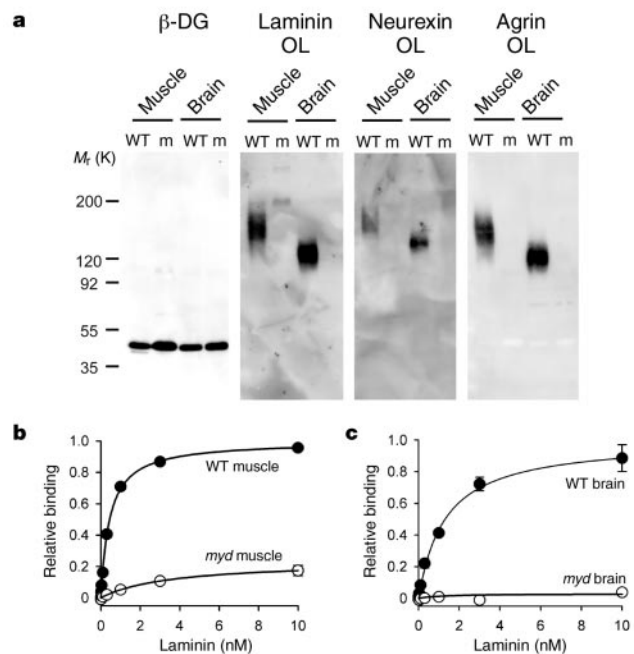

Figure 4 Dystroglycan–ligand interactions in *myd* muscle and brain. **a**, Ligand overlay (OL) assays on blots of WGA-enriched homogenates from *myd* skeletal muscle and brain. Lanes show control littermate mice (WT) and *myd* mice (m). **b**, **c**, Solid-phase laminin-binding assay in WT and *myd* WGA-enriched glycoproteins from skeletal muscle (**b**) and brain (**c**). A representative assay is shown with each binding condition performed in triplicate (mean ± s.d.).

skeletal muscle (not shown). Despite the differences in post-translational modification of α-DG in wild-type muscle and brain, the M_r of dystroglycan in *myd* muscle and brain is still slightly greater than the predicted M_r of the core protein (~75K).
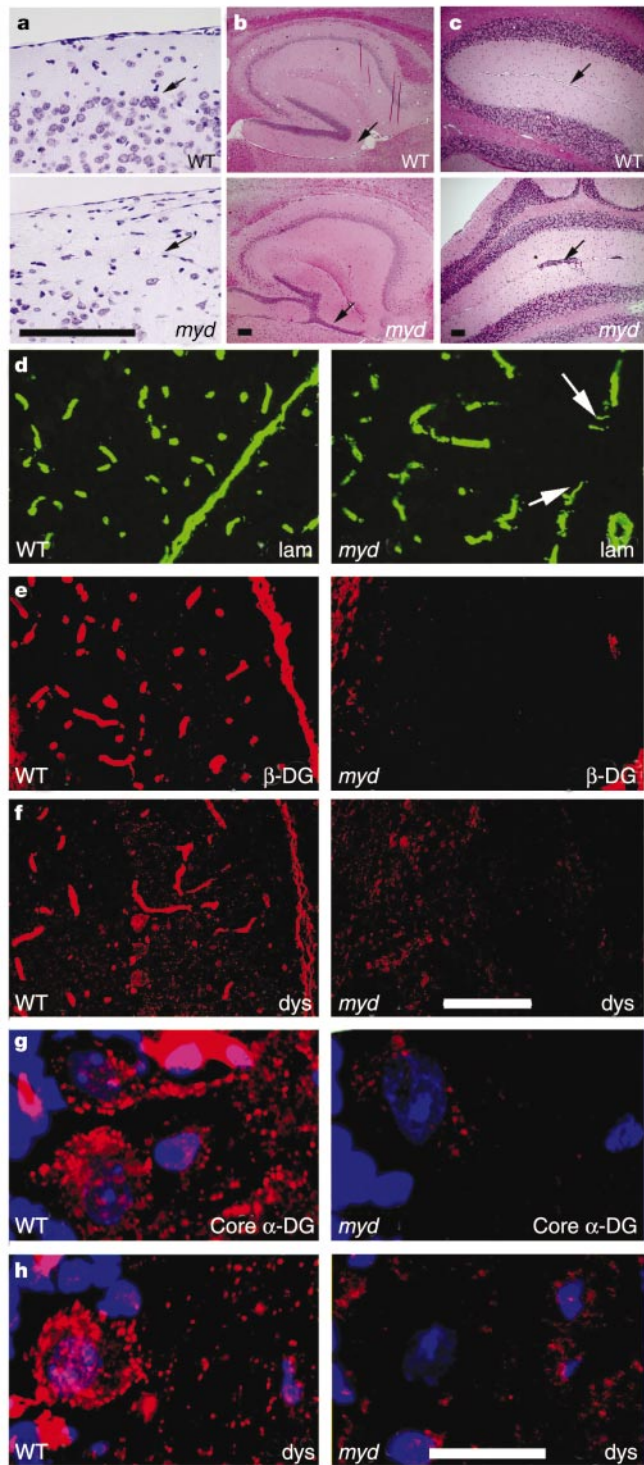

Figure 5 Abnormal neuronal migration and dystroglycan-associated protein targeting in *myd* mouse brain. **a**, Nissl-stained paired sagittal sections with boundaries between layer 1 and 2 in cerebral cortex (arrow). **b**, **c**, Abnormal migration of granule cells in *myd* dentate gyrus (**b**, arrow) and cerebellum (**c**, arrow). **d**, Polyclonal laminin (lam) antibody shows disruptions of glia-limiting membranes of cerebellum (arrows). **e**, **f**, Dystroglycan (**e**) and dystrophin (dys, **f**) targeting to cerebellar microvessels. **g**, **h**, Puncta staining with core α-DG (**g**) and dystrophin (**h**) antibodies in cerebellum (red). Counterstain is DAPI (blue). Scale bars: **a**–**f**, 100 μm; **g**, **h**, 20 μm.

Given that there were no previous reports of *myd* mice having brain abnormalities, we hypothesized that α-DG–ligand binding might be affected differently in *myd* muscle and brain than in MEB and FCMD muscle. However, ligand overlay assays showed that laminin, neurexin and agrin do not bind to α-DG from *myd* muscle and brain (Figs 3b and 4a). In addition, solid-phase binding assays of WGA-enriched glycoproteins show that high-affinity laminin binding is significantly reduced in *myd* muscle (Fig. 4b) and almost completely eliminated in *myd* brain (Fig. 4c). This suggests that the α-DG–ligand interactions are severely disrupted in *myd* mice, and that *myd* mice show a biochemical phenotype and M_r shift similar to MEB and FCMD patients.

Consistent with many of the brain abnormalities in MEB and FCMD patients, we show here that the *myd* mouse has a variety of neuronal migration abnormalities in cerebral cortex, cerebellum and hippocampus (Fig. 5). The cortical layering is disorganized, obscuring the well-defined boundary between layers I and II (Fig. 5a). The abnormal cortical layering is highly reminiscent of the type II lissencephalic changes seen in MEB and FCMD patients[21]. In cerebellum, populations of granule-cell neurons fail to migrate and are retained in clusters between adjacent folia (Fig. 5c). Granule-cell migration is also abnormal in hippocampus (Fig. 5b). The loss of α-DG–ligand interactions leads to several focal disruptions of glia-limiting basement membranes, noted by discontinuous laminin staining between adjacent folia in cerebellum (Fig. 5d). Furthermore, in contrast to *myd* muscle, which shows normal α2 laminin staining (not shown), α2 laminin staining is significantly reduced and pan-laminin antibodies show that laminin is mislocalized in cortex (not shown). In muscle, dystroglycan and DGC-associated proteins are expressed at the sarcolemma (see Supplementary Information). However, in brain the loss of the interactions between α-DG and the extracellular matrix leads to failure of α-DG, β-DG and dystrophin to concentrate to astrocyte foot processes (Fig. 5e, f, and Supplementary Information) and cerebellar puncta (Fig. 5g, h), although the expression of α-DG and β-DG appears similar in *myd* brain by western blot (Fig. 3b). Furthermore, proteins associated with DGC through dystrophin, including syntrophin and aquaporin-4, fail to target to the astrocyte foot process (see Supplementary Information). These results indicate that the loss of α-DG–ligand interactions disrupts the normal extracellular matrix composition and structure in important anchoring sites for supportive glial cells. Of equal importance, dystroglycan, through its interactions with extracellular ligands, seems to target proteins associated with the complex to the astrocyte foot process and the synapse.

The convergence of the post-translational perturbation and functional loss of α-DG–ligand interactions, muscular dystrophy and brain abnormalities in MEB, FCMD and *myd* mice provides strong evidence that α-DG is an important target protein that leads to disease. Importantly, the abnormal neuronal migration phenotype in *myd* mice is nearly identical to mice with a brain-specific dystroglycan gene deletion, demonstrating that the loss of dystroglycan–ligand binding activity is sufficient to account for this lissencephalic phenotype[22]. Indeed, the loss of dystroglycan–ligand binding activity in *myd* mice leads to a complete failure of targeting of dystroglycan and DGC proteins to important structural and function sites in brain, imparting a biochemical and functional dystroglycan deletion. These data provide strong support for the hypothesis that the tight link between the intracellular cytoskeleton and the extracellular environment through dystroglycan is central to the pathogenic mechanism of muscular dystrophy with abnormal neuronal migration.

The identification of an α-DG glycosylation defect in human MEB and FCMD patients highlights the importance of considering post-translational protein processing in genetic and acquired forms of human disease. Although fukutin belongs to the *fringe*-like family of glycosyltransferases, and LARGE has homology to an N-acetyl-

glucosamine transferase, neither has been demonstrated to have peptide transferase activity. Our results clearly show that a candidate glycoprotein substrate for these proteins shows a similar M_r shift with mutations in any of three distinct mammalian genes. This suggests that fukutin, LARGE and POMGnT1 may participate in a similar pathway that ultimately results in transfer of sugars to dystroglycan. Because *POMGnT1* is the only gene known to use *O*-linked mannosyl peptides as a substrate[4] (a sugar peptide linkage unique to α-DG[23]), we suggest that fukutin and LARGE may participate in either priming sugar donors for this reaction or cooperating with POMGnT1 in a larger macromolecular enzymatic complex. Finally, lymphocytic choriomeningitis virus (LCMV), which uses α-DG as a receptor, was recently shown to competitively inhibit α-DG interactions with laminin *in vitro*[24]. Transplacental fetal LCMV infection produces developmental abnormalities in the central nervous system remarkably similar to MEB and Walker–Warburg syndrome[25]. Therefore, disruption of dystroglycan–ligand interactions may be an important common mechanism to examine in a variety of genetic and acquired forms of neurological disorders that affect neuronal migration or synaptic integrity. □

Methods

Patient biopsies

Two siblings were diagnosed with Finnish MEB[21]. Genetic analysis of known mutated exons in *POMGnT1* revealed homozygosity for an IVS17 + 1 G-to-A splice site mutation previously described in the Turkish population[4]. One was a 2.5-year-old female with clinically diagnosed MEB or Walker–Warburg syndrome, based on the finding of congenital muscular dystrophy with eye and brain involvement. DNA for detailed genetic analysis was not available. The other was a 3.5-year-old male of Northern European and Slavic descent, with increased serum creatinine kinase, glaucoma, optic nerve colobomata/hypoplasia, abnormal T2 white matter and atrophy of the cerebellum and pons; he had a clinical diagnosis of MEB. The patient was heterozygous for a novel frameshift insertion in the tenth codon of exon 18 of *POMGnT1*. A second mutation was not found in known mutated exons 16–20 of *POMGnT1*, although a heterozygous polymorphism in intron 20 was observed. For MEB patients, control muscle was obtained from surgical discards of 12-year-old and 14-year-old females. FCMD patient tissue was obtained from three patients (aged 4–7 months) homozygous for retrotransposon insertions in the *fukutin* gene[3]. For FCMD patients, control muscle was from a 2.5-month-old sudden infant death syndrome patient, from the University of Miami Brain and Tissue Bank for Developmental Disorders. All tissue was obtained and tested in agreement with the Human Subjects Institutional Review Board of the University of Iowa.

Mice

Myodystrophy mice (*myd/myd*) and control littermate mice (+/+ or +/*myd*), 3–5 months old, were obtained from Jackson Laboratories.

Dystroglycan antibodies

VIA4-1 and IIH6 monoclonal antibodies recognizing α-DG were obtained from the University of Iowa Hybridoma Facility[6]. GT20ADG is from polyclonal antisera raised against the entire DGC[26] and purified against a hypoglycosylated full-length α-DG–human Fc fusion protein transiently expressed in HEK-293 cells[24]. AP83 is a rabbit polyclonal antibody raised against the carboxy-terminal 15 amino acids of β-DG[15].

Immunofluorescence microscopy

The primary antibodies for the DGC and laminin were used for immunofluorescence localization on human biopsies as described[27–29], and viewed on a Zeiss fluorescent microscope with digital imaging. For mouse brains, 7-μm cryosections were post-fixed in 2% paraformaldehyde; antibody blocking and labelling was performed in PBS with 0.5% Triton X-100 and 5% BSA. Histological staining (haematoxylin and eosin, Nissl) was performed on brains that were perfusion fixed and embedded in paraffin.

Glycoprotein enrichment and western blot analysis

One hundred milligrams of muscle biopsy were solubilized in 1 ml of Tris-buffered saline (TBS) containing 1% Triton X-100 and protease inhibitors. The solubilized fraction was incubated with 200 μl of WGA–agarose beads (Vector Labs) for 16 h. Pellets formed from the beads and these were washed three times in 1 ml TBS containing 0.1% Triton X-100 and protease inhibitors. The beads were then either directly boiled for 2 min in SDS–polyacrylamide gel electrophoresis (PAGE) loading buffer (western blotting, ligand overlay) or eluted with 1 ml TBS containing 0.1% Triton X-100, protease inhibitors and 300 mM *N*-acetyl-glucosamine (solid-phase binding assay). Proteins were separated by 3–15% SDS–PAGE and transferred to polyvinylidene fluoride (PVDF) membranes and probed with dystroglycan antibodies described above or monoclonal antibodies recognizing sarcoglycan isoforms (Novacastra), and developed with horseradish peroxidase (HRP)-enhanced chemiluminescence.

Ligand overlay assay

Ligand overlay assays were performed on PVDF membranes using mouse Engelbreth–Holm–Swarm (EHS) laminin, α-neurexin–immunoglobulin (Ig) fusion protein[19] or recombinant rat agrin (Chemicon). Briefly, PVDF membranes were blocked in laminin-binding buffer (LBB: 10 mM triethanolamine, 140 mM NaCl, 1 mM MgCl₂, 1 mM CaCl₂, pH 7.6) containing 5% nonfat dry milk (laminin or neurexin) or 5% BSA (agrin) followed by incubation of each ligand overnight at 4 °C in LBB. Membranes were washed and incubated with anti-laminin (Sigma) followed by anti-rabbit IgG–HRP, protein A–HRP (neurexin fusion protein) or anti-agrin (Chemicon) followed by anti-mouse IgG–HRP. Blots were developed by enhanced chemiluminescence (laminin and neurexin) or 4-chloro-1-naphthol (agrin).

Solid-phase assay

WGA eluates were diluted 1:50 in TBS and coated on polystyrene ELISA microplates (Costar) for 16 h at 4 °C. Plates were washed in LBB and blocked for 2 h in 3% BSA in LBB. Mouse EHS laminin was diluted in LBB and applied for 2 h. Wells were washed with 3% BSA in LBB, incubated for 30 min with 1:10,000 anti-laminin (Sigma) followed by anti-rabbit HRP. Plates were developed with *o*-phenylenediamine dihydrochloride and H₂O₂, reactions were stopped with 2N H₂SO₄, and values were obtained on a microplate reader. The data were fit to the equation $A = B_{max}x/(K_d + x)$, where K_d is the dissociation constant, A is absorbance, and B_{max} is maximal binding.

1. Dubowitz, V. Congenital muscular dystrophy: an expanding clinical syndrome. *Ann. Neurol.* **47**, 143–144 (2000); erratum *Ann. Neurol.* **47**, 554 (2000).
2. Toda, T. The Fukuyama congenital muscular dystrophy story. *Neuromuscul. Disord.* **10**, 153–159 (2000).
3. Kobayashi, K. *et al.* An ancient retrotransposal insertion causes Fukuyama-type congenital muscular dystrophy. *Nature* **394**, 388–392 (1998).
4. Yoshida, A. K. K. *et al.* Muscular dystrophy and neuronal migration disorder caused by mutations in a glycosyltransferase, POMGnT1. *Dev. Cell* **1**, 717–724 (2001).
5. Henry, M. D. & Campbell, K. P. Dystroglycan inside and out. *Curr. Opin. Cell Biol.* **11**, 602–607 (1999).
6. Ervasti, J. M. & Campbell, K. P. Membrane organization of the dystrophin–glycoprotein complex. *Cell* **66**, 1121–1131 (1991).
7. Ervasti, J. M. & Campbell, K. P. A role for the dystrophin–glycoprotein complex as a transmembrane linker between laminin and actin. *J. Cell Biol.* **122**, 809–823 (1993).
8. Ibraghimov-Beskrovnaya, O. *et al.* Primary structure of dystrophin-associated glycoproteins linking dystrophin to the extracellular matrix. *Nature* **355**, 696–702 (1992).
9. Ibraghimov-Beskrovnaya, O. *et al.* Human dystroglycan: skeletal muscle cDNA, genomic structure, origin of tissue specific isoforms and chromosomal localization. *Hum. Mol. Genet.* **2**, 1651–1657 (1993).
10. Hoffman, E. P., Brown, R. H. & Kunkel, L. M. Dystrophin: the protein product of the Duchenne muscular dystrophy locus. *Cell* **51**, 919–928 (1987).
11. Roberds, S. L. *et al.* Missense mutations in the adhalin gene linked to autosomal recessive muscular dystrophy. *Cell* **78**, 625–633 (1994).
12. Lim, L. E. *et al.* β-sarcoglycan: characterization and role in limb-girdle muscular dystrophy linked to 4q12. *Nature Genet.* **11**, 257–265 (1995).
13. Noguchi, S. *et al.* Mutations in the dystrophin-associated protein γ-sarcoglycan in chromosome 13 muscular dystrophy. *Science* **270**, 819–822 (1995).
14. Nigro, V. *et al.* Autosomal recessive limb-girdle muscular dystrophy, LGMD2F, is caused by a mutation in the δ-sarcoglycan gene. *Nature Genet.* **14**, 195–198 (1996).
15. Williamson, R. A. *et al.* Dystroglycan is essential for early embryonic development: disruption of Reichert's membrane in Dag1-null mice. *Hum. Mol. Genet.* **6**, 831–841 (1997).
16. Henry, M. D. & Campbell, K. P. A role for dystroglycan in basement membrane assembly. *Cell* **95**, 859–870 (1998).
17. Gee, S. H., Montanaro, F., Lindenbaum, M. H. & Carbonetto, S. Dystroglycan-α, a dystrophin-associated glycoprotein, is a functional agrin receptor. *Cell* **77**, 675–686 (1994).
18. Campanelli, J. T., Roberds, S. L., Campbell, K. P. & Scheller, R. H. A role for dystrophin-associated glycoproteins and utrophin in agrin-induced AChR clustering. *Cell* **77**, 663–674 (1994).
19. Sugita, S. *et al.* A stoichiometric complex of neurexins and dystroglycan in brain. *J. Cell Biol.* **154**, 435–445 (2001).
20. Grewal, P. K., Holzfeind, P. J., Bittner, R. E. & Hewitt, J. E. Mutant glycosyltransferase and altered glycosylation of α-dystroglycan in the myodystrophy mouse. *Nature Genet.* **28**, 151–154 (2001).
21. Haltia, M. Muscle-eye-brain disease: a neuropathological study. *Ann. Neurol.* **41**, 173–180 (1997).
22. Moore, S. A. *et al.* Deletion of brain dystroglycan recapitulates aspects of congenital muscular dystrophy. *Nature* **418**, 422–425 (2002).
23. Chiba, A. *et al.* Structures of sialylated O-linked oligosaccharides of bovine peripheral nerve α-dystroglycan. The role of a novel O-mannosyl-type oligosaccharide in the binding of α-dystroglycan with laminin. *J. Biol. Chem.* **272**, 2156–2162 (1997).
24. Kunz, S., Sevilla, N., McGavern, D. B., Campbell, K. P. & Oldstone, M. B. Molecular analysis of the interaction of LCMV with its cellular receptor α-dystroglycan. *J. Cell Biol.* **155**, 301–310 (2001).
25. Barton, L. L. & Mets, M. B. Congenital lymphocytic choriomeningitis virus infection: decade of rediscovery. *Clin. Infect. Dis.* **33**, 370–374 (2001).
26. Jung, D. *et al.* Characterization of δ-sarcoglycan, a novel component of the oligomeric sarcoglycan complex involved in limb-girdle muscular dystrophy. *J. Biol. Chem.* **271**, 32321–32329 (1996).
27. Engvall, E. *et al.* Mapping of domains in human laminin using monoclonal antibodies: localization of the neurite-promoting site. *J. Cell Biol.* **103**, 2457–2465 (1986).
28. Matsumura, K. *et al.* Deficiency of the 50K dystrophin-associated glycoprotein in severe childhood autosomal recessive muscular dystrophy. *Nature* **359**, 320–322 (1992).
29. Allamand, V. *et al.* Mild congenital muscular dystrophy in two patients with an internally deleted laminin α2-chain. *Hum. Mol. Genet.* **6**, 747–752 (1997).

Deletion of brain dystroglycan recapitulates aspects of congenital muscular dystrophy

Steven A. Moore*, **Fumiaki Saito**†, **Jianguo Chen**‡, **Daniel E. Michele**†, **Michael D. Henry**†, **Albee Messing**§, **Ronald D. Cohn**† **Susan E. Ross-Barta***, **Steve Westra***, **Roger A. Williamson**||, **Toshinori Hoshi**‡ **& Kevin P. Campbell**†

* *Department of Pathology;* † *Howard Hughes Medical Institute, Department of Physiology and Biophysics and Department of Neurology;* ‡ *Department of Physiology and Biophysics; and* || *Department of Obstetrics and Gynecology, The University of Iowa, Iowa City, Iowa 52242-1101, USA*
§ *Waisman Center and Department of Pathobiological Sciences, University of Wisconsin, Madison, Wisconsin 53705-2280, USA*

Fukuyama congenital muscular dystrophy (FCMD), muscle–eye–brain disease (MEB), and Walker–Warburg syndrome are congenital muscular dystrophies (CMDs) with associated developmental brain defects[1–4]. Mutations reported in genes of FCMD[2] and MEB[5] patients suggest that the genes may be involved in protein glycosylation. Dystroglycan is a highly glycosylated component of the muscle dystrophin–glycoprotein complex[6] that is also expressed in brain, where its function is unknown[7]. Here we show that brain-selective deletion of dystroglycan in mice is sufficient to cause CMD-like brain malformations, including disarray of cerebral cortical layering, fusion of cerebral hemispheres and cerebellar folia, and aberrant migration of granule cells. Dystroglycan-null brain loses its high-affinity binding to the extracellular matrix protein laminin, and shows discontinuities in the pial surface basal lamina (glia limitans) that probably underlie the neuronal migration errors. Furthermore, mutant mice have severely blunted hippocampal long-term potentiation with electrophysiologic characterization indicating that dystroglycan might have a postsynaptic role in learning and memory. Our data strongly support the hypothesis that defects in dystroglycan are central to the pathogenesis of structural and functional brain abnormalities seen in CMD.

The dystrophin–glycoprotein complex (DGC) of striated muscle is a well-characterized array of cytoplasmic, membrane-spanning and extracellular proteins that form a critical linkage between the cytoskeleton and the basal lamina[8]. The central protein linking DGC to the basal lamina is dystroglycan, a high-affinity receptor for several proteins (for example, laminin, agrin, neurexin and perlecan) that is composed of α- and β- subunits encoded by a single gene[6,9]. α-dystroglycan (α-DG) is a highly glycosylated extracellular component, whereas β-DG spans the plasma membrane forming a

bridge between α-DG and the cytoskeleton[6]. Within the central nervous system (CNS), dystroglycan is abundant at two basal lamina interfaces formed by astrocytes: foot processes abutting on cerebral blood vessels, and foot processes that constitute the glia limitans at the pial surface of the brain and spinal cord[7]. Brain dystroglycan has also been localized to neuronal elements in several locations, including hippocampus and cerebellar cortex, where it may form a structural element of certain synapses[7].

To explore the function of dystroglycan in brain and to determine whether dystroglycan operates in the pathogenesis of brain abnormalities such as those seen in CMD, we used Cre-*loxP* methodology to selectively delete dystroglycan from the CNS. Brain-selective expression of Cre recombinase was accomplished using a human glial fibrillary acid protein (GFAP) promoter expressed as early as embryonic day 13.5 (ref. 10). Studies in reporter mice reveal expression in astrocytes, oligodendroglia, ependyma and a large proportion of neurons[10]. It is likely that the human GFAP promoter is transiently active in neural progenitor cells, resulting in Cre recombination of floxed genes (genes flanked by *loxP* elements) that persist for the lifetime of several CNS cell lineages.

We produced both GFAP-Cre/DG$^{lox/−}$ and GFAP-Cre/DG$^{lox/lox}$ (GFAP-Cre/DG-null) mice that at weaning fit the expected mendelian distribution of each genotype. GFAP-Cre/DG-null mice are fertile and have no gross neurological abnormalities. Dystroglycan is largely absent from CNS tissue of GFAP-Cre/DG-null mice (Fig. 1a
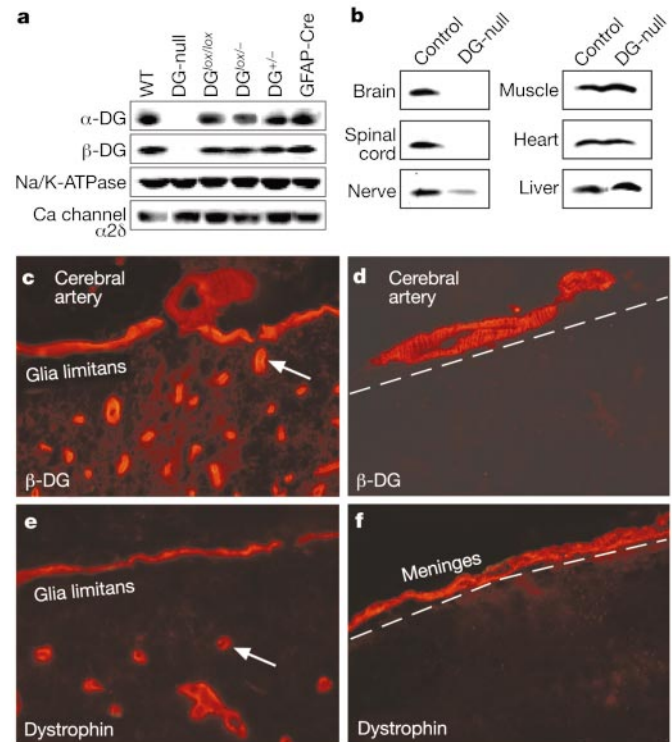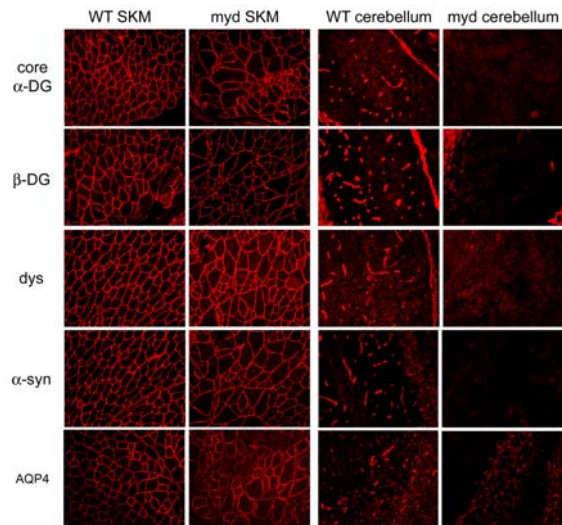

Figure 1 Tissue-selective deletion of dystroglycan. **a**, Western blot analysis of brain. WT, wild type; DG-null, GFAP-Cre/DG-null; DG$^{+/−}$, heterozygous dystroglycan null; DG$^{lox/−}$, heterozygous floxed/dystroglycan-null; DG$^{lox/lox}$, homozygous floxed. **b**, Western blot with a β-DG antibody. **c**, β-DG immunofluorescence of control cerebral cortex shows staining of smooth muscle in a small cerebral artery on the pial surface and astrocyte foot processes along the glia limitans and cerebral microvessels (arrow points to one microvessel). **d**, β-DG immunofluorescence is retained in only a small cerebral artery on the surface of DG-null cerebrum. **e**, Dystrophin immunofluorescence parallels that of β-DG in control brain. **f**, Dystrophin immunofluorescence is retained only in vessels of the meninges of DG-null brain. The position of the unstained glia limitans is marked by a dashed white line in **d** and **f**.

Supplemental Experimental Procedures

Supplemental Figure 1. Immunofluorescence localization of DGC and DGC
associated proteins in myd skeletal muscle and brain. Skeletal muscle from
myd mice shows normal sarcolemma localization of DG, dystrophin, α-
syntrophin and aquaporin 4. Aquaporin 4 is only lost in a subpopulation of
actively regenerating fibers. However, in myd brain (cerebellum is shown),
DG and dystrophin fail to localize at astrocyte foot processes around
microvessels and at limiting membranes. In addition, aquaporin 4 (which
binds to α-syntrophin), and α-syntrophin (which binds to dystrophin) fails to
localize the foot processes around microvessels.